ADVANCED FUNCTIONAL MATERIALS
www.afm-journal.de

Amine-Free Synthesis of Cesium Lead Halide Perovskite Quantum Dots for Efficient Light-Emitting Diodes

*Emre Yassitepe, Zhenyu Yang, Oleksandr Voznyy, Younghoon Kim, Grant Walters, Juan Andres Castañeda, Pongsakorn Kanjanaboos, Mingjian Yuan, Xiwen Gong, Fengjia Fan, Jun Pan, Sjoerd Hoogland, Riccardo Comin, Osman M. Bakr, Lazaro A. Padilha, Ana F. Nogueira, and Edward H. Sargent**

Cesium lead halide perovskite quantum dots (PQDs) have attracted significant interest for optoelectronic applications in view of their high brightness and narrow emission linewidth at visible wavelengths. A remaining challenge is the degradation of PQDs during purification from the synthesis solution. This is attributed to proton transfer between oleic acid and oleylamine surface capping agents that leads to facile ligand loss. Here, a new synthetic method is reported that enhances the colloidal stability of PQDs by capping them solely using oleic acid (OA). Quaternary alkylammonium halides are used as precursors, eliminating the need for oleylamine. This strategy enhances the colloidal stability of OA capped PQDs during purification, allowing us to remove excess organic content in thin films. Inverted red, green, and blue PQD light-emitting diodes (LED) are fabricated for the first time with solution-processed polymer-based hole transport layers due to higher robustness of OA capped PQDs to solution processing. The blue and green LEDs exhibit threefold and tenfold improved external quantum efficiency (EQE), respectively, compared to prior related reports for amine/ammonium capped cross-linked PQDs. The brightest blue LED based on all inorganic $CsPb(Br_{1-x}Cl_x)_3$ PQDs is also reported.

1. Introduction

Solution-processed hybrid and inorganic lead halide perovskites are of interest for optoelectronic applications because of their excellent photophysical and transport properties.[1–3] Methylammonium and formamidinium lead halide ($MAPbX_3$, $FAPbX_3$, X = Cl, Br, I) perovskites are top contenders in solution-processed single junction solar cells, having recently passed the 22% certified power conversion efficiency milestone.[1,3] Organic lead halide perovskites are also explored in photodetectors,[4–6] lasing applications,[7,8] and light-emitting diodes (LEDs).[9–11]

Rapid advances in bulk perovskite materials have in turn brought significant attention to quantum dots based on perovskites. Colloidal organic metal halide perovskite nanomaterials were reported based on $MAPbBr_3$ nanocrystals obtained via a recrystallization process.[12] A hot injection synthesis method was then developed to generate fully inorganic $CsPbX_3$ perovskite quantum dots (PQDs)[13–15] that showed narrow photoluminescence (PL) spectra and high photoluminescence quantum yields (PLQY) that reached 90%. Furthermore, $MAPbX_3$ PQDs were reported with PLQY of 70% and a wide color gamut.[16] $CsPbX_3$ PQDs have particularly wide-ranging quantum-size-effect tunability in light of their large exciton Bohr radius and halide compositional tuning.

To date, colloidal perovskite nanocrystal syntheses have adopted lead halides as the source for lead and halogens, a strategy similar to that used to prepare bulk perovskite materials. This requires dissolution of PbX_2 salts in a polar medium such as dimethylformamide (DMF), and it also demands the use of a mixture of oleylamine and oleic acid (OA) as surfactants.[12,16–18]

Dr. E. Yassitepe, Dr. Z. Yang, Dr. O. Voznyy, Dr. Y. Kim, G. Walters, Dr. P. Kanjanaboos,[+] Dr. M. Yuan, X. Gong, Dr. F. Fan, Dr. S. Hoogland, Dr. R. Comin, Prof. E. H. Sargent
Department of Electrical and Computer Engineering
University of Toronto
10 King's College Road, Toronto, Ontario M5S 3G4, Canada
E-mail: ted.sargent@utoronto.ca
Dr. E. Yassitepe, Prof. A. F. Nogueira
Instituto de Química
Universidade Estadual de Campinas (UNICAMP)
Caixa Postal: 6154, 13083-970 Campinas, São Paulo, Brazil

DOI: 10.1002/adfm.201604580

Dr. J. A. Castañeda, Prof. L. A. Padilha
Instituto de Fisica "Gleb Wataghin"
UNICAMP
P.O. Box 6165, 13083-859 Campinas
Sao Paulo, Brazil
Dr. J. Pan, Prof. O. M. Bakr
Solar and Photovoltaic Engineering Research Center
King Abdullah University of Science and Technology (KAUST)
23955-6900 Thuwal, Saudi Arabia

[+]Present address: Materials Science and Engineering, Faculty of Science, Mahidol University, 272 Rama 6 Rd., Ratchathewi District, Bangkok, 10400, Thailand

A nonpolar solvent method was reported for $CsPbX_3$ PQDs in which PbX_2 salts were solubilized in oleylamine/OA capping agents in a noncoordinating solvent, 1-octadecene (ODE), followed by injection of cesium oleate at elevated temperatures (140–200 °C).[13] However, these PQDs exhibited poor colloidal stability and readily precipitated from the crude solution.[13,19–21] Recently, Hens and co-workers explained the reasons for the limited stability of PQDs, attributing it to facile proton exchange between the oleate and amine surfactants. This leads to a dynamic equilibrium between bound and unbound ligands, enabling facile ligand loss.[22] In addition, oleylamine itself can also accelerate the degradation of the nanocrystals by coordinating the lead species (Pb-oleate, PbX_2) and ultimately dissolving the lead oleate Z-type ligands from the surface.[23]

For these reasons, a new synthetic strategy is urgently needed to overcome the reliance on oleylamine and the requirement of multiple competitive ligands. Moving beyond the use of oleylamine is challenging because this ligand is presently relied upon to solubilize the lead halide precursor. We thus turned instead to Cs-oleate (CsOA) and Pb-oleate ($PbOA_2$) and searched for a new halide source. We were inspired by ligand exchanges in chalcogenide quantum dots. Tetrabutylammonium iodide (TBAI) is used to provide stable iodide passivation of metal-rich QD surfaces through the cleavage of lead-carboxylate bonds in proton-donating solvents (e.g., methanol).[24–27] This exchange mechanism provides a predictive pathway for the reaction between CsOA and $PbOA_2$ with quaternary alkylammonium halide salts (NR_4X, R = alkyl group).

Recently, Wei et al. reported a room-temperature synthetic method based on carboxylic acid capped $CsPbBr_3$ PQDs and further applied postsynthetic anion exchange techniques to form $CsPbX_3$ PQDs (X = Cl, Br, I).[28] However, PQDs show degraded PLQY properties within 2–3 days and, surprisingly, suffered from lower PLQY for above room temperature reactions. Here, we carry out an extensive study to employ OA capping supported by experimental studies and theoretical investigations. We demonstrate an amine-free synthesis that utilizes tetraoctylammonium halides (TOAX) for preparation of OA-capped $CsPbX_3$ PQDs without the need of post-anion exchange methods. The PQDs show PLQY up to 70%, narrow emission spectra, and enhanced colloidal stability. We show that these PQDs are more stable upon purification with polar solvents, an advance that we attribute to stronger ligand attachment. We further fabricate red, green, and blue (RGB) PQD LED using first time solution-processed polymer-based hole transport layers in an inverted LED structure for PQDs. Green and blue LEDs show a threefold increase in performance for green, and tenfold for blue LED efficiencies compared to prior related reports for amine/ammonium-capped cross-linked PQDs.[14] We further explore, using ultrafast spectroscopy, the effects of photocharging and fast Auger recombination in PQDs. We identify these as the key factors that need to be addressed to achieve further improvements in LED performance.

2. Results and Discussion

To understand the reaction mechanism, its limiting steps, and possible ways to control growth, we carried out density functional theory molecular dynamics simulations of the

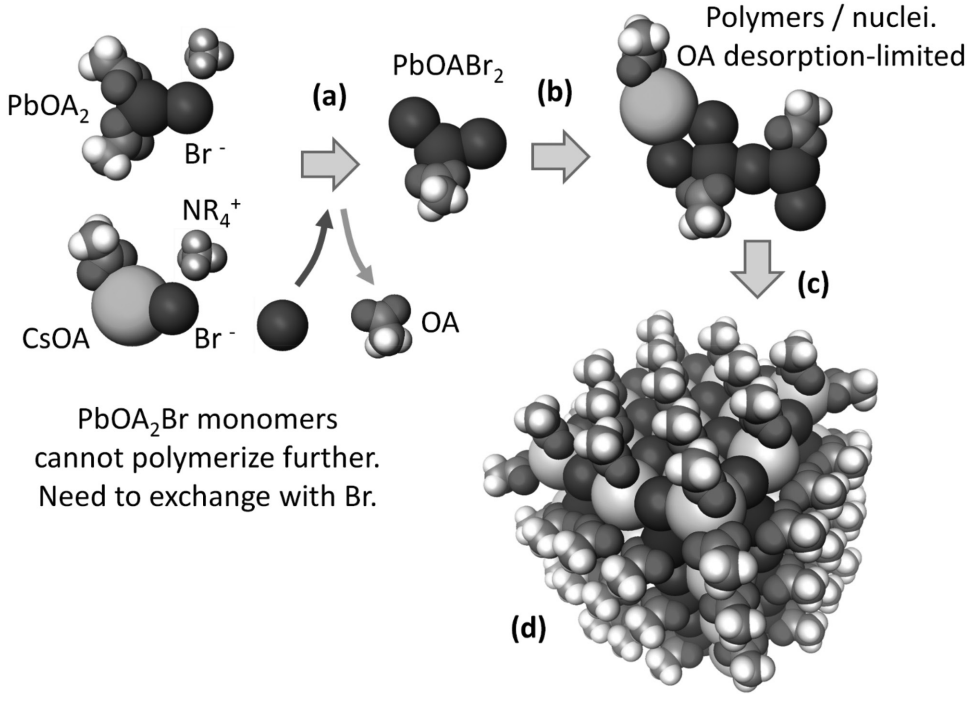

Figure 1. Density functional theory molecular dynamics simulation of $CsPbBr_3$ nucleation and growth steps (for simplicity, the synthesis is shown with acetate group instead of oleate). a) Dissociated ammonium bromide ions form complexes with CsOA and $PbOA_2$. b) Further reaction between these complexes requires one of the OA^- being replaced with Br^-. c) Br-enriched Cs and Pb complexes polymerize through multicoordinated Br. d) $CsPbBr_3$ nanocrystal passivated with OA ligands.

Adv. Funct. Mater. **2016**,
DOI: 10.1002/adfm.201604580

nucleation and crystal growth kinetics starting from the chosen precursors: CsOA, $Pb(OA)_2$, and TOABr (for simplicity, the acetate molecule is shown in the figure instead of oleic acid). In the first step of the reaction, we find that Cs and Pb oleates react readily with Br anions, since Cs and Pb cations are large and prefer higher coordination than OA can provide (**Figure 1**a). However, the resulting ($PbOA_2Br$) clusters do not react further as they become electronically saturated, even though the size of the cation could allow for higher coordination. In contrast, both $PbBr_2$ and ($PbOABr_2$) are more reactive and form polymeric chains, thanks to the ability of Br^- to coordinate to more than one lead ion (Figure 1b). The exchange of the oleate ion for a bromide anion therefore becomes the limiting step for further growth of the nuclei. It is known that the detachment of the oleate anion from the surface of the lead cation is highly unfavorable unless a proton participates and assists the detachment.[12] Similarly, detachment of oleate ligands continues to be the limiting step at every stage of the nanocrystal growth (Figure 1c). Instead of a proton, we use TOA cation to facilitate the desorption of OA and to control the nanocrystal growth. The use of TOA eliminates formation of reversible amine–ammonium species due to the absence of proton. However, when alkylammonium halides are used, there can be reversible exchange between alkylammonium to alkyamine. Therefore, TOA eliminates species for amine formation.

In a typical reaction, Cs-acetate, Pb-acetate, ODE, oleic acid are placed in the flask and heated to 120 °C until CsOA and $PbOA_2$ are formed under vacuum. Then, the flask is placed under nitrogen and the temperature is lowered to 75 °C to inject the TOAX source. Injection of TOABr at 75 °C into a CsOA and $PbOA_2$-containing mixture resulted in an immediate change in the color of the solution from colourless and transparent to green, indicating the formation of $CsPbBr_3$ PQDs. Moreover, the solution remained clear longer than conventionally prepared PQDs, indicating that the oleic acid capped dots show enhanced colloidal stability (Figure S1, Supporting Information). This was also confirmed during purification of the PQDs by attempting to crash the crude solution without any antisolvents. To our surprise, oleic acid capped dots do not precipitate without the introduction of an antisolvent, whereas conventionally prepared PQDs precipitate spontaneously from solution.[13,20,21] $CsPbBr_3$ and $CsPb(Br,Cl)_3$ PQDs showed high

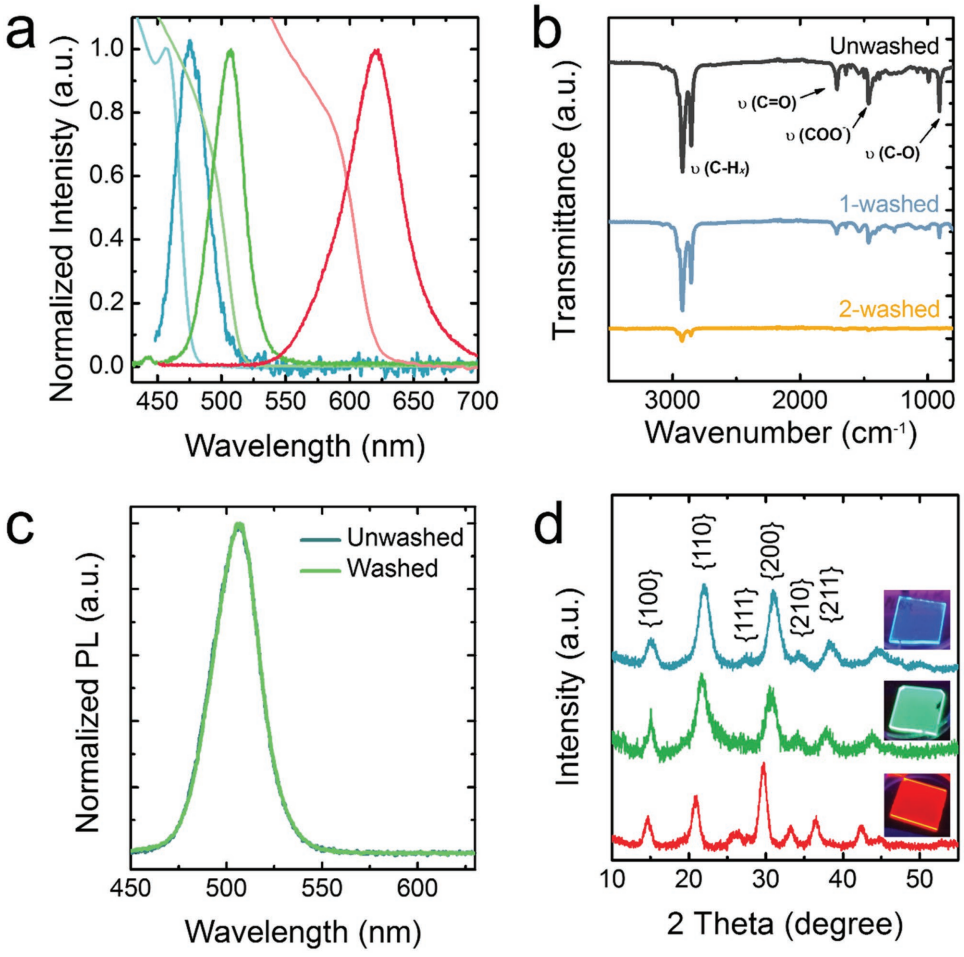

Figure 2. Optical and structural characterization of $CsPbX_3$ (X = Cl, Br, I) PQDs. a) Absorption and PL spectra of RGB $CsPbX_3$ PQDs color coded with the corresponding color. b) FTIR spectra of unwashed, once-washed, and twice-washed $CsPbBr_3$ PQDs. c) PL spectra of unwashed and twice-washed $CsPbBr_3$ PQDs showing identical PL spectrum. d) X-ray powder diffraction of $CsPb(Br_{3-x}Cl_x)$, $CsPbBr_3$, and $CsPb(Br_{3-x}I_x)$ PQDs confirming cubic perovskite structure.

stability; however, $CsPb(Br,I)_3$ PQDs do become unstable over time. This may be attributed to their sensitivity to moisture. The synthesis of blue and red photoluminescent PQDs is achieved by the incorporation of mixed halide anions and carried out in a similar fashion to $CsPbBr_3$ PQDs (e.g., Br/Cl and Br/I) (**Figure 2**a).

The absence of oleylamine also accelerates the growth reaction of PQDs. For example, the growth of average $CsPbBr_3$ (≈8 nm) PQDs requires ≈150 °C reaction temperature, whereas in the absence of oleylamine, similar-sized PQDs were formed at 75 °C. We attributed the lower reaction temperature to the absence of oleylamine, already known by its strong coordination that reduces the reactivity of PbX_2. This inhibiting effect had also been reported for syntheses of InP quantum dots when oleylamine was utilized.[29] We further studied the effect of oleylamine on as-prepared $CsPbBr_3$ PQDs by observing them with PL spectroscopy (Figure S2, Supporting Information). We find that addition of increasing quantities of oleylamine causes a blue shift, indicating surface etching or oxidation over time.

Fourier transform infrared (FTIR) spectra of as-synthesized PQDs show the presence of OA (COOH) and oleate species (COO^-) **(**Figure 2b**)**. COO^- stretching confirmed the binding of Pb-oleate species on PQD surfaces at 1525 and 1553 cm^{-1} (Figure S3, Supporting Information).[30] These signals confirm the bond chelating and bridging from $PbOA_2$ on the surfaces of oleic acid capped PbS nanoparticles.[30] As a result of the subsequent washing step, PQDs maintained surface-bound COO^- groups, and their solutions possessed a lower quantity of free OA. This allowed us to remove most excess ligands without affecting the colloidal stability. The PQD PL peak positions are not shifted (Figure 2c). In conventional oleylamine/oleic acid capped PQDs, a similar degree of purification inevitably led to a red shift of PL, indicating growth or fusion of those PQDs.[21] X-ray diffraction measurements confirm the cubic perovskite crystal structure of RGB PQDs with peak shifts consistent with the formation of alloys (Figure 2d).

We utilized X-ray photoelectron spectroscopy (XPS) to monitor the presence of amine and ammonium ligands on the surface of PQDs after one- and two-time washing. Both amine and ammonium species are present on the surface of conventional PQDs even after two washing steps. This resonates with the conclusions of Hens and co-workers regarding ready and reversible proton transfer between OA and amine, which accelerates the desorption of protonated OA or amine-coordinated $PbOA_2$ Z-type ligands and eventually causes the degradation of PQDs.[22,23,31] High resolution XPS N1s spectra of our solely oleic acid capped $CsPbBr_3$ PQDs do not show any detectable nitrogen after one and two washing steps (Figure S4, Supporting Information), confirming the absence of amine and ammonium species.

High-resolution transmission electron microscopy (HR-TEM) imaging of $CsPbBr_3$ quantum dots confirms the $CsPbBr_3$ perovskite structure (**Figure 3**a). The lattice spacing (5.8 Å) corresponds to the {110} lattice planes. HR-TEM analysis shows that average particle size is between 7 and 10 nm, confirming

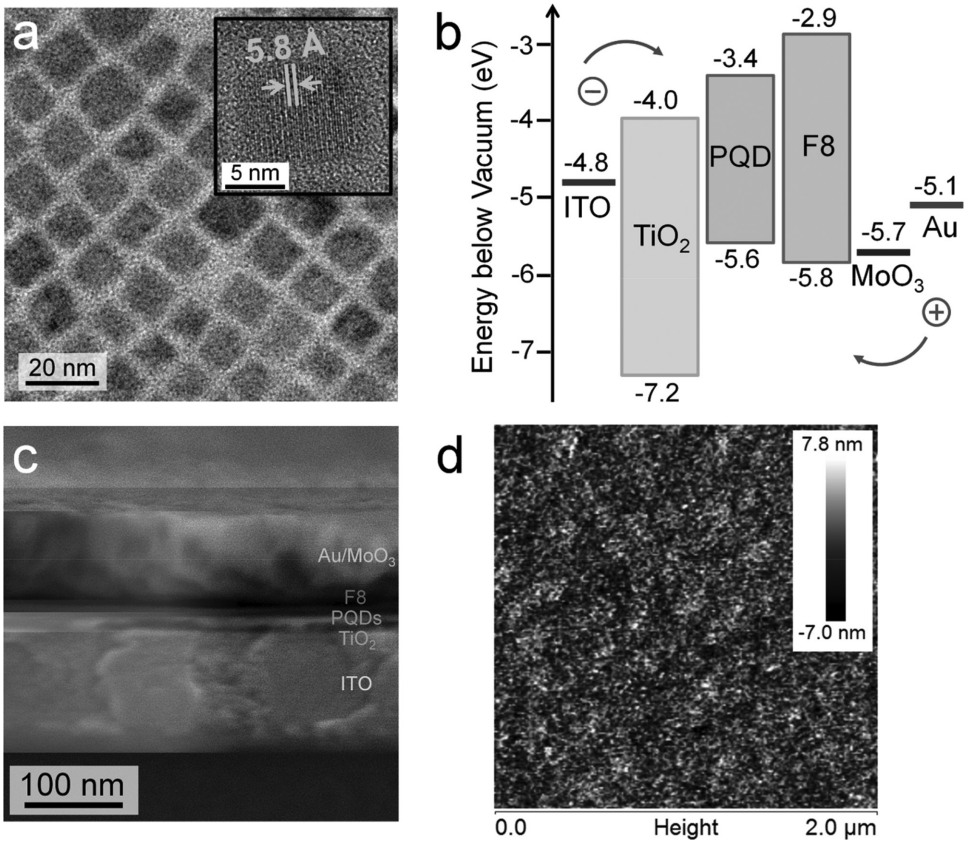

Figure 3. a) High resolution TEM image of $CsPbBr_3$ PQDs, inset showing d-spacing calculation for single crystal. b) Device band diagram, c) Cross-sectional SEM image of $CsPbBr_3$ PQD-LED. d) AFM image of $CsPbBr_3$ PQD emission layer on top of TiO_2.

Adv. Funct. Mater. **2016**,
DOI: 10.1002/adfm.201604580

the quantum confinement effect (Figure S5, Supporting Information). Interestingly, the reaction carried out at 75 °C does not form platelets, a finding that had previously been reported for oleylamine/oleic acid based PQDs with reaction temperatures of 90–130 °C.[32]

Ligand detachment during washing steps enabled PQDs to attach firmly onto hydrophilic substrates. An inverted LED device architecture was chosen in which the perovskite quantum dot layer was sandwiched by a TiO_2 electron transport layer and by a poly(9,9′-dioctylfluorence) (F8) hole transport layer. The band diagram of the devices, shown in Figure 3b, indicates the well-aligned band levels between PQDs and charge transport layers. Cross-section scanning electron microscope (SEM) imaging revealed that the overall thickness of the device is less than 200 nm (TiO_2: 10–15 nm, active perovskite layer: ≈10 nm, F8: 15 nm, MoO_3/Au anode: ≈100 nm) (Figure 3c). Atomic force microscopy (AFM) confirmed the low surface roughness (R_q) of the active layer (on top of TiO_2/ITO (Indium Tin Oxide) substrate) was around 2 nm (Figure 3d).

RGB electroluminescence (EL) was achieved by fabricating devices with the corresponding types of perovskite quantum dots (red: Br/I mixed; green: pure Br; blue: Br/Cl mixed). Compared to the PL spectra (**Figure 4**a), no significant EL wavelength shift was observed in RGB devices (EL peak at ≈650, 510, 495 nm, respectively). Blue and green EL signals are symmetric without noticeable peak broadening (full width at half maximum of RGB devices are 35, 25, and 21 nm, respectively), indicating that the luminescence qualities of the active perovskite quantum dots were well-preserved during solution-processed device fabrication.

Device turn-on voltages were between 2.6 and 4 V depending on the PQD type (Figure 4d). The corresponding peak external quantum efficiency (EQE) values are 0.05%, 0.325%, and 0.075% for RGB devices, respectively (Figure 4c). Green and blue LEDs show a threefold increase in performance for green, and tenfold for blue LED efficiencies compared to prior related reports for amine/ammonium capped cross-linked PQDs. The relatively low EQE value of the blue-emitting device arises from inefficient charge blocking by the F8 layer. The conduction band of perovskite was moved closer to the lowest unoccupied molecular orbital (LUMO) of F8, which is also reflected in the device current density–voltage (*J*–*V*) response (Figure 4b). We summarize PQD-LED performance published to date and device architectures in Table S1 (Supporting Information). All published PQD-LEDs utilize evaporated electron or hole transport layers. Here, we report a new device architecture that

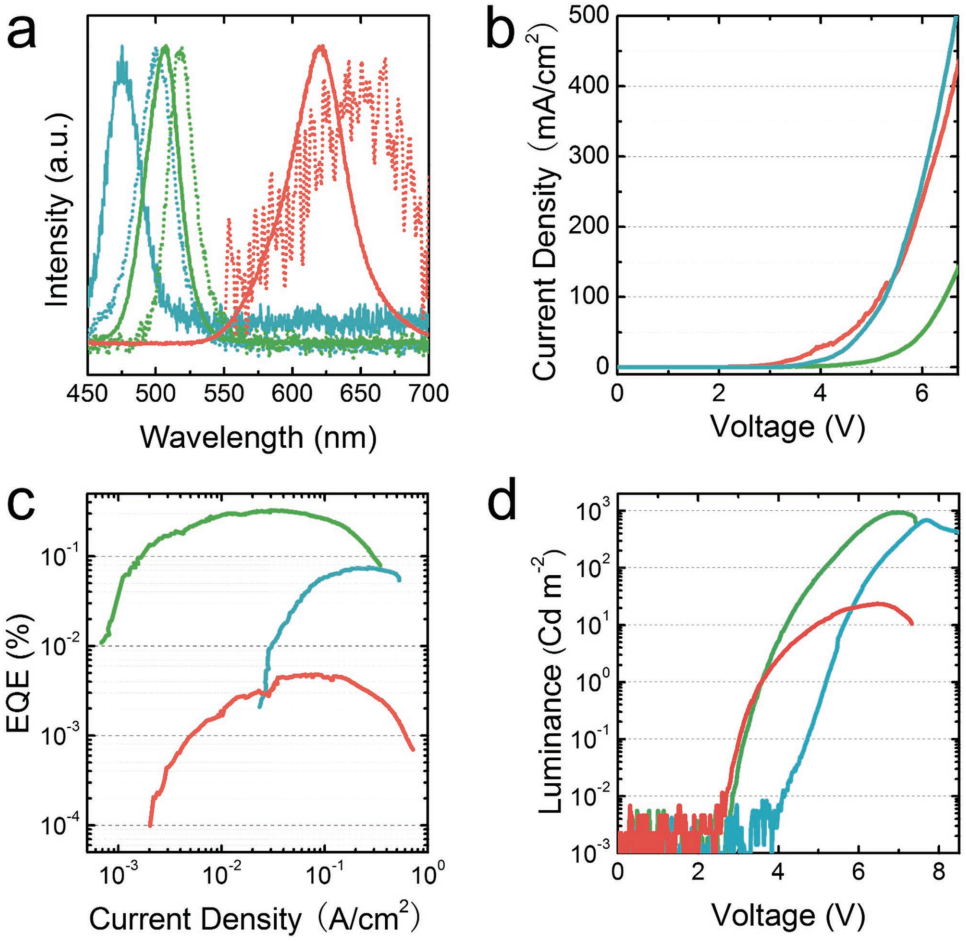

Figure 4. Device characterization of RGB PQD-LEDs. a) RGB photoluminescence (straight lines) and electroluminescence (dashed lines). b) Current density versus voltage (*J*–*V*) curves of PQD-LEDs. c) EQE versus current density plots for RGB PQD-LEDs. d) Luminance versus voltage curves for RGB PQD-LEDs.

utilizes a solution-processed polymer-based hole transport layer due to robustness of OA capped PQDs to solution processing. $CsPbX_3$ PQDs provide LED device performance comparable with previous reports (Table S1, Supporting Information). The range of the luminance was 30–930 cd m^{-2}, comparable to previous PQD LEDs (Figure 4d).[14,33] It was, however, achieved at notably lower voltage (R: 2.6 V, G: 2.8 V, and B: 4.1 V). Although almost the same brightness was found from the blue and green devices, we noticed the red-emitting devices were dimmer: their lower performance may be attributed to the higher air and moisture sensitivity of $CsPb(Br_{3-x}I_x)$ PQDs.

A possible reason for the limited EQE in PQD-based LEDs is the strong influence of Auger-assisted nonradiative decay, which could be a result of charged PQDs due to uncontrolled charge injection, and consequent trion decay.[34] To verify the strength of Auger recombination in these materials, we performed a series of transient absorption (TA) studies in solution and films. **Figure 5** shows TA results for the green-emitting PQDs with a biexciton lifetime of 38 ± 5 ps. To verify that the fast decay is indeed due to biexciton formation, we characterized its amplitude as a function of the pump intensity (see Figure S6, Supporting Information), finding that it follows Poisson statistics expected for biexcitons. A slower decay of about 180 ps also emerges as the pump intensity increases, indicating the presence of ionized PQDs and trion decay.[35] These values agree with the values recently reported for similar $CsPbBr_3$ PQDs.[36,37] For the sample investigated in this work, photoionization and consequent trion formation accounts for less than 10% of the measured signal. However, when comparing the TA results for PQDs in solution and in spin-cast films, we observed a stronger influence of this charged species in films. We expect photocharging to be a slow and cumulative process.[38] This is suggestive that charging could be one factor that limits the device's EQE. Considering the PL and trion lifetimes, we can estimate that, if the device is dominated by charged species, the maximum EQE would be near 3%. This suggests that it is imperative to develop engineered PQD heterostructures that can reduce trion formation.

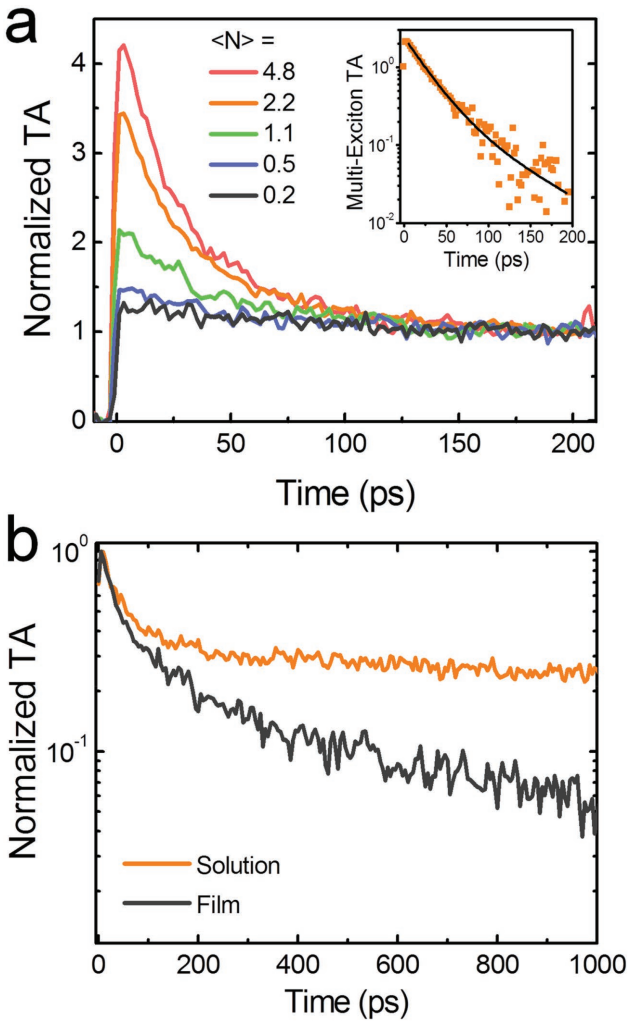

Figure 5. a) Transient absorption spectra for green-emitting PQDs in toluene solution for several pump intensities (inset shows the multiexciton dynamics at high excitation energy ($\langle N \rangle = 2.2$)). b) Comparison between the transient absorption spectra of PQDs in solution and film.

3. Conclusion

We developed an amine-free synthesis for PQDs stabilized solely by oleic acid, enabled by the choice of a novel halide precursor. Oleic acid capped PQDs showed improved colloidal stability and provided high stability against polar solvents during purification. This allows solution-processed conductive PQD films with low organic content and increased stability. We report a new LED device architecture by utilizing a solution-processed polymer-based hole transport layer with highly comparable RGB LED performances. Further optimization of the synthesis and device fabrication of perovskite quantum dots is the subject of ongoing investigation, in particular, the core–shell structures to reduce the Auger recombination losses.

Supporting Information

Supporting Information is available from the Wiley Online Library or from the author.

Acknowledgements

E.Y., Z.Y., and O.V. contributed equally to this work. This publication was based in part on work supported by the Award KUS-11-009-21, made by the King Abdullah University of Science and Technology (KAUST), by the Ontario Research Fund – Research Excellence Program, and by the Natural Sciences and Engineering Research Council of Canada (NSERC). E.Y. acknowledges support from FAPESP-BEPE (2014/18327-9) and FAPESP (2013/05798-0) fellowships. E.Y. acknowledges LNnano-CNPEM (TEM-19813) for high resolution TEM facility. J.A.C. and L.A.P. acknowledge the financial support from FAPESP (Project number 2013/16911-2). A.F.N. acknowledges FAPESP, CNPq, and INEO. The authors thank Dr. Y. Zhao for useful discussions. The authors thank L. Levina, E. Palmiano, R. Wolowiec, and D. Kopilovic for their technical help over the course of this study.

Received: September 4, 2016
Published online:

[1] W. Nie, H. Tsai, R. Asadpour, J.-C. Blancon, A. J. Neukirch, G. Gupta, J. J. Crochet, M. Chhowalla, S. Tretiak, M. A. Alam, H.-L. Wang, A. D. Mohite, *Science* **2015**, *347*, 522.
[2] Z. Ning, X. Gong, R. Comin, G. Walters, F. Fan, O. Voznyy, E. Yassitepe, A. Buin, S. Hoogland, E. H. Sargent, *Nature* **2015**, *523*, 324.
[3] J. Burschka, N. Pellet, S.-J. Moon, R. Humphry-Baker, P. Gao, M. K. Nazeeruddin, M. Grätzel, *Nature* **2013**, *499*, 316.
[4] M. I. Saidaminov, V. Adinolfi, R. Comin, A. L. Abdelhady, W. Peng, I. Dursun, M. Yuan, S. Hoogland, E. H. Sargent, O. M. Bakr, *Nat. Commun.* **2015**, *6*, 8724.
[5] Y. Fang, Q. Dong, Y. Shao, Y. Yuan, J. Huang, *Nat. Photonics* **2015**, *9*, 679.
[6] L. Dou, Y. Micheal Yang, J. You, Z. Hong, W.-H. Chang, G. Li, Y. Yang, *Nat. Commun.* **2014**, *5*, 5404.
[7] G. Xing, N. Mathews, S. S. Lim, N. Yantara, X. Liu, D. Sabba, M. Grätzel, S. Mhaisalkar, T. C. Sum, *Nat. Mater.* **2014**, *13*, 476.
[8] F. Deschler, M. Price, S. Pathak, L. E. Klintberg, D.-D. Jarausch, R. Higler, S. Hüttner, T. Leijtens, S. D. Stranks, H. J. Snaith, M. Atatüre, R. T. Phillips, R. H. Friend, *J. Phys. Chem. Lett.* **2014**, *5*, 1421.
[9] Z.-K. Tan, R. S. Moghaddam, M. L. Lai, P. Docampo, R. Higler, F. Deschler, M. Price, A. Sadhanala, L. M. Pazos, D. Credgington, F. Hanusch, T. Bein, H. J. Snaith, R. H. Friend, *Nat. Nanotechnol.* **2014**, *9*, 687.
[10] G. Li, Z.-K. Tan, D. Di, M. L. Lai, L. Jiang, J. H.-W. Lim, R. H. Friend, N. C. Greenham, *Nano Lett.* **2015**, *15*, 2640.
[11] J. Wang, N. Wang, Y. Jin, J. Si, Z.-K. Tan, H. Du, L. Cheng, X. Dai, S. Bai, H. He, Z. Ye, M. L. Lai, R. H. Friend, W. Huang, *Adv. Mater.* **2015**, *27*, 2311.
[12] L. C. Schmidt, A. Pertegás, S. González-Carrero, O. Malinkiewicz, S. Agouram, G. Mínguez Espallargas, H. J. Bolink, R. E. Galian, J. Pérez-Prieto, *J. Am. Chem. Soc.* **2014**, *136*, 850.
[13] L. Protesescu, S. Yakunin, M. I. Bodnarchuk, F. Krieg, R. Caputo, C. H. Hendon, R. X. Yang, A. Walsh, M. V. Kovalenko, *Nano Lett.* **2015**, *15*, 3692.
[14] J. Song, J. Li, X. Li, L. Xu, Y. Dong, H. Zeng, *Adv. Mater.* **2015**, *27*, 7162.
[15] J. Pan, S. P. Sarmah, B. Murali, I. Dursun, W. Peng, M. R. Parida, J. Lu, L. Sinatra, N. Alyami, C. Zhao, E. Alarousu, T. K. Ng, B. S. Ooi, O. M. Bakr, O. F. Mohammed, *J. Phys. Chem. Lett.* **2015**, *6*, 5027.
[16] F. Zhang, H. Zhong, C. Chen, X. Wu, X. Hu, H. Huang, J. Han, B. Zou, Y. Dong, *ACS Nano* **2015**, *9*, 4533.
[17] X. Li, Y. Wu, S. Zhang, B. Cai, Y. Gu, J. Song, H. Zeng, *Adv. Funct. Mater.* **2016**, *26*, 2435.
[18] K.-H. Wang, L. Wu, L. Li, H.-B. Yao, H.-S. Qian, S.-H. Yu, *Angew. Chem., Int. Ed.* **2016**, *55*, 8328.
[19] O. Vybornyi, S. Yakunin, M. V. Kovalenko, *Nanoscale* **2016**, *8*, 6278.
[20] S. Yakunin, L. Protesescu, F. Krieg, M. I. Bodnarchuk, G. Nedelcu, M. Humer, G. De Luca, M. Fiebig, W. Heiss, M. V. Kovalenko, *Nat. Commun.* **2015**, *6*, 8056.
[21] Y. Kim, E. Yassitepe, O. Voznyy, R. Comin, G. Walters, X. Gong, P. Kanjanaboos, A. F. Nogueira, E. H. Sargent, *ACS Appl. Mater. Interfaces* **2015**, *7*, 25007.
[22] J. De Roo, M. Ibáñez, P. Geiregat, G. Nedelcu, W. Walravens, J. Maes, J. C. Martins, I. Van Driessche, M. V. Kovalenko, Z. Hens, *ACS Nano* **2016**, *10*, 2071.
[23] N. C. Anderson, M. P. Hendricks, J. J. Choi, J. S. Owen, *J. Am. Chem. Soc.* **2013**, *135*, 18536.
[24] Z. Ning, O. Voznyy, J. Pan, S. Hoogland, V. Adinolfi, J. Xu, M. Li, A. R. Kirmani, J.-P. Sun, J. Minor, K. W. Kemp, H. Dong, L. Rollny, A. Labelle, G. Carey, B. Sutherland, I. Hill, A. Amassian, H. Liu, J. Tang, O. M. Bakr, E. H. Sargent, *Nat. Mater.* **2014**, *13*, 822.
[25] J. Tang, K. W. Kemp, S. Hoogland, K. S. Jeong, H. Liu, L. Levina, M. Furukawa, X. Wang, R. Debnath, D. Cha, K. W. Chou, A. Fischer, A. Amassian, J. B. Asbury, E. H. Sargent, *Nat. Mater.* **2011**, *10*, 765.
[26] P. Schapotschnikow, B. Hommersom, T. J. H. Vlugt, *J. Phys. Chem. C* **2009**, *113*, 12690.
[27] C.-H. M. Chuang, P. R. Brown, V. Bulović, M. G. Bawendi, *Nat. Mater.* **2014**, *13*, 796.
[28] S. Wei, Y. Yang, X. Kang, L. Wang, L. Huang, D. Pan, *Chem. Commun.* **2016**, *52*, 7265.
[29] P. M. Allen, B. J. Walker, M. G. Bawendi, *Angew. Chem., Int. Ed.* **2010**, *49*, 760.
[30] L. C. Cass, M. Malicki, E. A. Weiss, *Anal. Chem.* **2013**, *85*, 6974.
[31] A. Hassinen, I. Moreels, K. De Nolf, P. F. Smet, J. C. Martins, Z. Hens, *J. Am. Chem. Soc.* **2012**, *134*, 20705.
[32] Y. Bekenstein, B. A. Koscher, S. W. Eaton, P. Yang, A. P. Alivisatos, *J. Am. Chem. Soc.* **2015**, *137*, 16008.
[33] J. Pan, L. N. Quan, Y. Zhao, W. Peng, B. Murali, S. P. Sarmah, M. Yuan, L. Sinatra, N. M. Alyami, J. Liu, E. Yassitepe, Z. Yang, O. Voznyy, R. Comin, M. N. Hedhili, O. F. Mohammed, Z. H. Lu,D. H. Kim, E. H. Sargent, O. M. Bakr, *Adv. Mater.* **2016**, *28*, 8718.
[34] W. K. Bae, Y.-S. Park, J. Lim, D. Lee, L. A. Padilha, H. McDaniel, I. Robel, C. Lee, J. M. Pietryga, V. I. Klimov, *Nat. Commun.* **2013**, *4*, 2661.
[35] L. A. Padilha, J. T. Stewart, R. L. Sandberg, W. K. Bae, W.-K. Koh, J. M. Pietryga, V. I. Klimov, *Nano Lett.* **2013**, *13*, 1092.
[36] N. S. Makarov, S. Guo, O. Isaienko, W. Liu, I. Robel, V. I. Klimov, *Nano Lett.* **2016**, *16*, 2349.
[37] J. A. Castañeda, G. Nagamine, E. Yassitepe, L. G. Bonato, O. Voznyy, S. Hoogland, A. F. Nogueira, E. H. Sargent, C. H. Brito Cruz, L. A. Padilha, *ACS Nano* **2016**, *10*, 8603.
[38] L. A. Padilha, I. Robel, D. C. Lee, P. Nagpal, J. M. Pietryga, V. I. Klimov, *ACS Nano* **2011**, *5*, 5045.